Some remarks on model structures

It is the author's opinion that the proliferation of model structures in the biopyriboles has got completely out of hand. Numerous different formulations exist, and the complexity of this topic far exceeds the complexity of the natural structures. Model building should be a pragmatic occupation; if it's not useful, don't do it.

The Tetrahedral Double Chain in Non-^{iv}Al Amphiboles

There are considerable stereochemical variations in the tetrahedral double-chain from structure to structure. This is presumably in response to the differing local environments and has led to examination of the double-chain element in terms of various models of bonding.

From a molecular orbital viewpoint, several predictions can be made concerning the stereochemistry of polymerized tetrahedra (Brown *et al.* 1969, Gibbs *et al.* 1972): (i) Si–O(nbr) bonds are usually shorter than Si–O(br) bonds, providing the Si–O(br)–Si angle is not wide and $\overline{\chi}$ (the mean electronegativity of the nontetrahedral cations) is not large; (ii) the shorter Si–O(br) bonds are usually associated with the wider Si–O(br)–Si angles, with Si–O(br) an inverse function of cos(Si–O(br)–Si); (iii) tetrahedral angles usually decrease in the order O(nbr)–Si–O(nbr) > O(nbr)–Si–O(br) > O(br)–Si–O(br), and (iv) Si–O bond lengths are a function of the O–Si–O angles in which they are involved. These predictions provide a framework within which the variations in tetrahedral stereochemistry may be examined.

Bond-valence models are related to the fact that deviations from Pauling's second rule (Pauling 1929, 1960) are correlated with variations in cation-anion distances in structures. Several schemes that relate bond lengths to bond valences have been developed; of these, the treatments of Baur (1970, 1971) and Brown & Shannon (1973) are the more general. Baur (1971) has derived an equation relating Si–O bond length to the deviation from the mean bond-strength sum of all anions co-ordinating a specific Si exhibited by a specific anion. This equation may be used both to predict individual bond-lengths absolutely from a forecast mean bond-length, or it may be used in conjunction with the observed mean bond-length to predict deviations from that mean. Brown & Shannon (1973) have derived curves relating bond length to bond valence. Although the curves are not immediately predictive as is the scheme of Bauer (1970, 1971), they recognize weak bonding interactions that are either ignored or overemphasized in the previous method. Additional bond-valence curves, including some for the F anion, have been presented by Brown & Wu (1976) and Brown (1978). Both these methods are of considerable use in the interpretation of the detailed stereochemistry of the amphiboles.

The C2/m amphiboles

There are two unique cation-sites with pseudo-tetrahedral co-ordination in this structure type, the T(1) and T(2) sites. Figure 11 shows the details of their co-ordination. Both sites have point-symmetry 1 and are surrounded by four oxygen anions. The T(1) tetrahedron shares one corner with an adjacent T(1) tetrahedron, one corner with an adjacent T(2) tetrahedron, one corner with the other adjacent T(2) tetrahedron and with a [6]-co-ordinate M(4) polyhedron, and the fourth corner with the M(1), M(2) and M(3) octahedra; in addition, it shares one edge with an [8]-co-ordinate M(4) polyhedron. The T(2) tetrahedron shares one corner with an adjacent T(1) tetrahedron, one corner with the other adjacent T(1) tetrahedron and with an [8]-co-ordinate M(4) polyhedron, one corner with the M(2) octahedron and a fourth corner with the M(1), M(2) and M(4) polyhedra; in addition, it shares one edge with the M(4) polyhedron.

Brown & Gibbs (1969, 1970) examined the steric details in the double chains of four $C2/m$ amphiboles and showed that they conform to the predictions of the molecular orbital model; in addition, they correlated individual Si–O bond lengths with $\overline{\chi}$ (the mean electronegativity of the nontetrahedral cations). This approach was developed further by Mitchell *et al.* (1971), who presented equations relating the T–O(nbr) bond lengths to <T–O(br)–T> and $\overline{\chi}$:

$$\text{T(1)–O(1)} = 1.137 + 0.0029\langle\text{T–O(5, 6, 7)–T}\rangle + 0.051\overline{\chi}_{\text{O(1)}}$$

$$\text{T(2)–O(2)} = 1.211 + 0.0029\langle\text{T–O(5, 6)–T}\rangle + 0.007\overline{\chi}_{\text{O(2)}}$$

$$\text{T(2)–O(4)} = 1.213 + 0.0026\langle\text{T–O(5, 6)–T}\rangle + 0.009\overline{\chi}_{\text{O(4)}}$$

A comparison of the bond lengths calculated from these equations with the observed values for the $C2/m$ amphiboles is given in Figure 30. Mitchell *et al.* (1971) also showed that the T(2)–O(br) distances vary inversely with both T(2)–O(2) and T(2)–O(4). Assuming that the average bond-order of an Si–O bond in an SiO_4 tetrahedron is 1.5 and using the equation

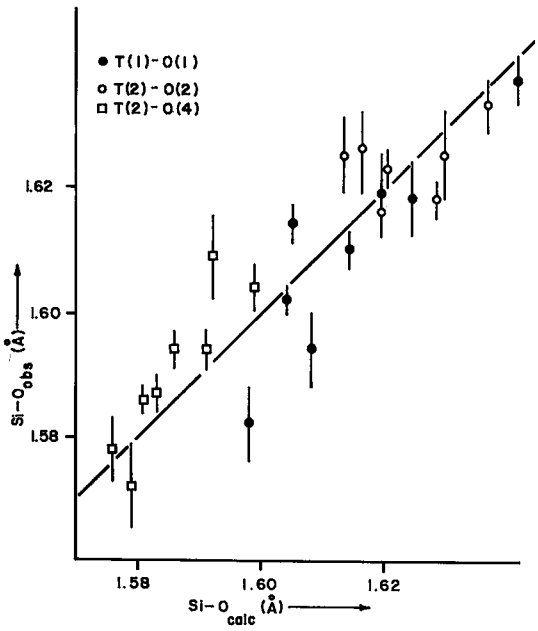

FIG. 30. Comparison of the T–O (nbr) bonds in non-^{iv}Al amphiboles, calculated from the equations of Mitchell *et al.* (1971), with the corresponding observed values; vertical lines through each data-point represent±1 standard deviation.

of Robinson (1963) relating bond order to bond length, irregular tetrahedra that are characterized by large differences between their individual Si–O bond-lengths will have a larger <Si–O> bond-length than more regular tetrahedra. Figure 31 shows a plot of the estimated standard deviation of <T–O> *versus* <T–O>; a linear trend is definitely apparent, supporting the above argument, but the correlation is not as marked as that originally shown by Mitchell *et al.* (1971) with the smaller data-set then available.

It is of interest to examine further some of these relationships with the larger data-set now available. Figure 32 shows the variation in the grand <T–O(br)> with both grand <T–O(br)–T> and $-1/\cos$<T–O(br)–T>; as the total variation in <T–O(br)–T> is only ~8°, the nonlinearity in grand <T–O(br)> as a function of grand <T–O(br)–T> is not apparent; the excellent correlations support the contentions of Brown & Gibbs (1969, 1970) and Mitchell *et al.* (1971). However, if <T–O(br)> is examined as a function of <T–O(br)–T> for all bridging anions individually (Fig. 33), the excellent correlation disappears, although individual trends for each anion can be discerned. The nonsystematic behavior in the individual trends can be directly related to the sizes of the cations in

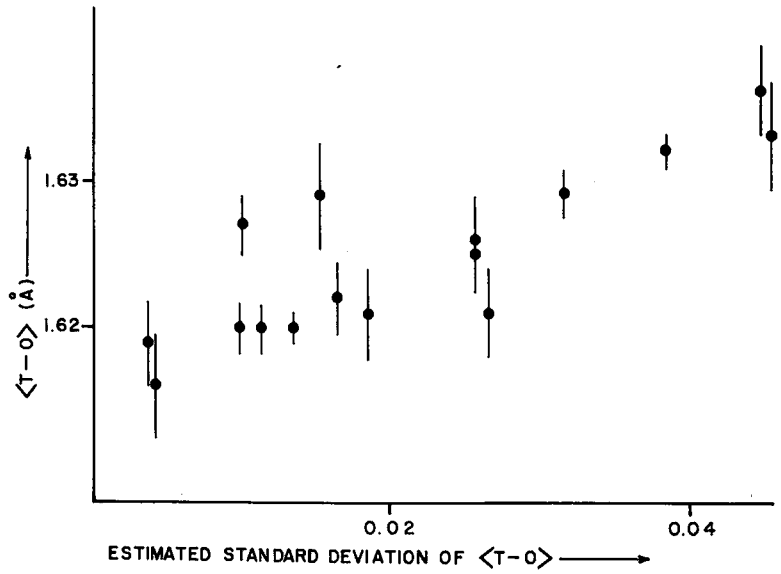

FIG. 31. Variation in <T–O> as a function of its standard deviation (calculated from the individual T–O bond-lengths) for $C2/m$ amphiboles with little or no ^{iv}Al [modified after Mitchell *et al.* (1971)].

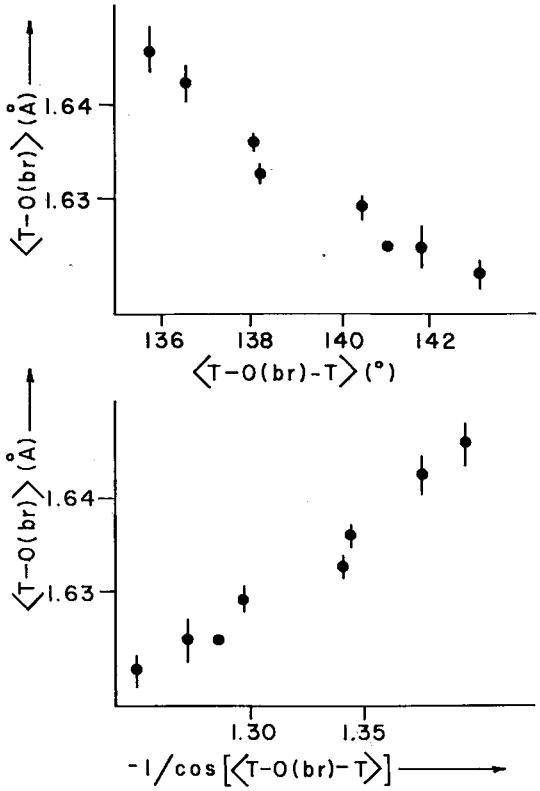

FIG. 32. Variation in grand <T–O(br)> as a function of grand <T–O(br)–T> for the $C2/m$ amphiboles with ^{IV}Al less than 0.10 a.p.f.u. The variation in <T–O(br)–T> is not sufficient to show the nonlinearity inherent in the upper graph.

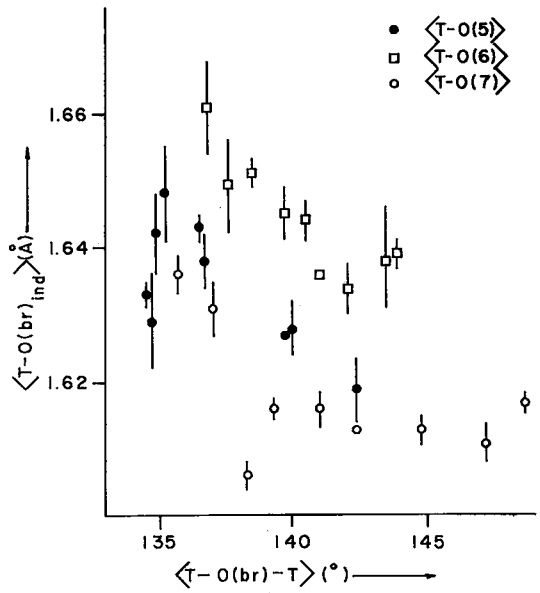

FIG. 33. Variation in individual <T–O(br)> as a function of the <T–O(br)–T> angle for the $C2/m$ amphiboles with ^{IV}Al less than 0.10 a.p.f.u.

the octahedral strip. This is particularly noticeable in glaucophane(26), where <T–O(5)> or T(1)–O(5)–T(2) (or both) are "anomalously" short because they are involved in a linkage to the small M(2) octahedron. Detailed stepwise regression analyses show that individual <T–O(br)> bonds are not significantly correlated with the mean electronegativity of the nontetrahedral cations bonded to the tetrahedral group (Hawthorne 1973). Figure 34 shows the variation in T–O as a function of $<O–T–O>_3$; the overall correlation is marked and agrees with the predictions of Gibbs *et al.* (1972), but considerable scatter occurs. The correlations for individual bonds are generally better developed than that of the graph as a whole, suggesting that the ideal relationship is definitely perturbed by the crystal field.

Cameron & Gibbs (1973) performed E.H.M.O. calculations for tremolite(30) and fluor-tremolite(36), and noted that the observed bond-

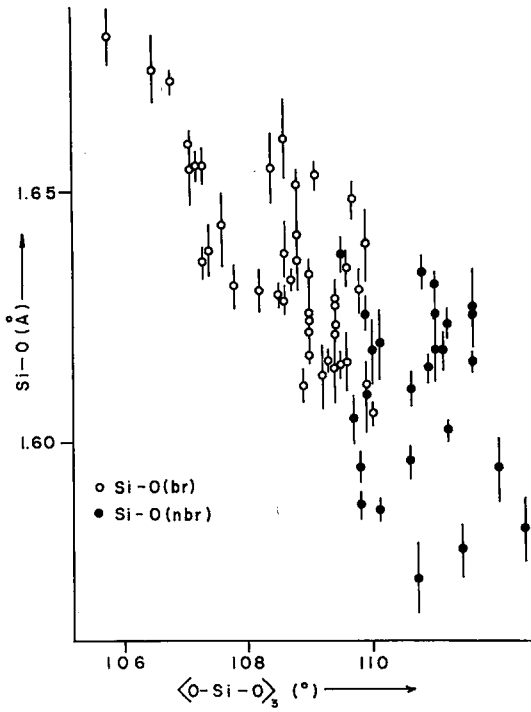

FIG. 34. Variation in individual Si–O bond-lengths as a function of the mean value of the three O–Si–O angles involved in that bond for the $C2/m$ amphiboles with ^{IV}Al less than 0.10 a.p.f.u.

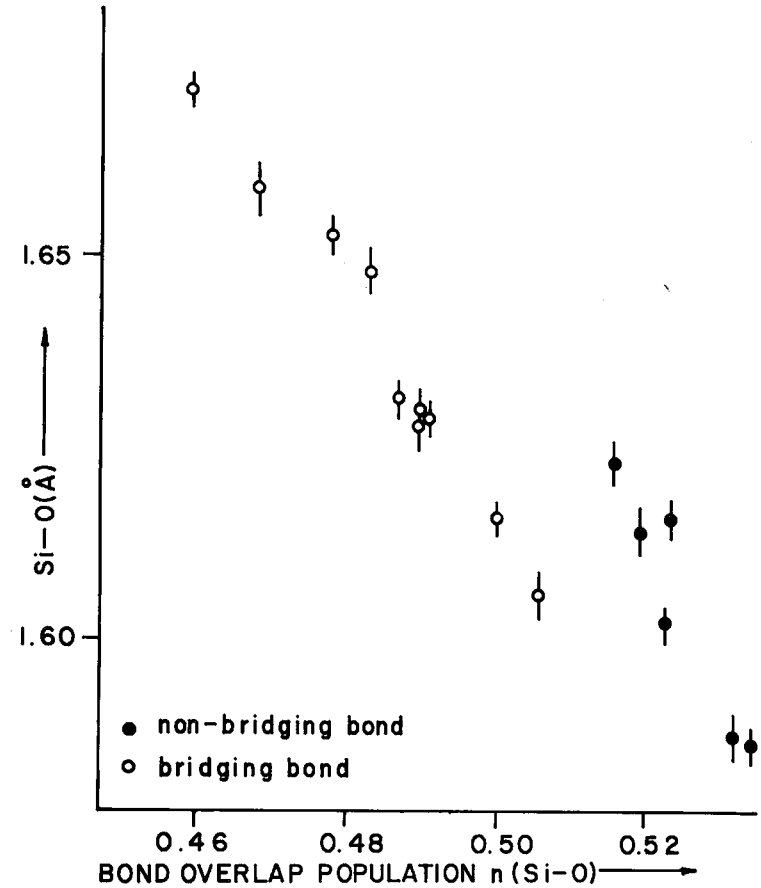

FIG. 35. Variation in observed Si–O bond-lengths for tremolite(30) and fluor-tremolite(36) as a function of bond-overlap population calculated using extended Hückel molecular-orbital theory [after Cameron & Gibbs (1973)].

lengths are inversely correlated with the Si–O bond-overlap populations (Fig. 35). Although a valence-basis set was used for these calculations, the Si–O(br) and Si–O(nbr) seem to form two separate populations (*cf.* Gibbs *et al.* 1972). In a series of calculations for idealized orthosilicic acid molecules, Louisnathan & Gibbs (1972) found that the bond-overlap population is non-linearly correlated with O–Si–O angles involved in the bond. This correlation varies with differing molecular orbital environments along the basal-apical bond-directions, and can be rationalized in terms of changes in the nonequivalent hybridization characteristics of the central Si atom. Thus the presence of two ordered populations in Figure 35 is not inconsistent with the conclusion of Gibbs *et al.* (1972) that at least part of the Si–O bond-length variations observed in silicates can be rationalized in terms of a covalent bonding model.

Before any systematic analysis of Si–O distances can be made using the scheme of Baur (1970, 1971), it is necessary to assign co-ordination numbers to the O(5) and O(6) anions. This problem in the amphiboles is discussed in more detail in the section on the M(4) site. Here, an M(4) co-ordination of [6] will be used for the iron–magnesium–manganese amphiboles and an M(4) co-ordination of [8] will be used for all other $C2/m$ amphiboles. A comparison of the observed and calculated bond-lengths is given in Table 18 and Figure 36. The agreement with the observed values is much the same for each method, with a grand mean deviation of 0.01 Å. This indicates that the amphiboles obey the extended electrostatic

TABLE 18. COMPARISON OF OBSERVED TETRAHEDRAL BOND-LENGTHS WITH VALUES CALCULATED FROM THE METHOD OF BAUR (1971)* FOR EIGHT C2/m AMPHIBOLES WITH $^{IV}Al \leq 0{\cdot}10$apfu

		(21)	(22)	(26)	(28)	(30)	(34)	(35)	(36)
T(1)-O(1)	obs	1.619	1.637(4)	1.618(6)	1.610(3)	1.602(2)	1.582(6)	1.594(6)	1.614(3)
	(1)	1.612	1.612	1.630	1.612	1.613	1.623	1.623	1.613
	(2)	1.611	1.619	1.622	1.612	1.609	1.605	1.605	1.609
T(1)-O(5)	obs	1.614	1.627(5)	1.616(7)	1.622(4)	1.632(2)	1.625(6)	1.636(7)	1.628(3)
	(1)	1.612	1.612	1.626	1.612	1.635	1.648	1.648	1.635
	(2)	1.611	1.619	1.618	1.612	1.631	1.630	1.630	1.631
T(1)-O(6)	obs	1.628	1.630(4)	1.621(6)	1.633(3)	1.629(2)	1.641(7)	1.624(7)	1.630(4)
	(1)	1.650	1.650	1.626	1.650	1.635	1.648	1.648	1.635
	(2)	1.649	1.657	1.618	1.650	1.631	1.630	1.630	1.631
T(1)-O(7)	obs	1.613	1.613(2)	1.611(3)	1.616(2)	1.616(1)	1.636(3)	1.631(4)	1.606(2)
	(1)	1.612	1.612	1.615	1.612	1.613	1.638	1.638	1.613
	(2)	1.611	1.619	1.607	1.612	1.609	1.620	1.620	1.609
<T(1)-O>	obs	1.619	1.627	1.616	1.620	1.620	1.621	1.621	1.622
	(1)	1.620	1.620	1.624	1.620	1.624	1.639	1.639	1.624
T(2)-O(2)	obs	1.625	1.633(4)	1.618(6)	1.618(3)	1.616(2)	1.625(6)	1.626(7)	1.623(3)
	(1)	1.624	1.624	1.628	1.624	1.620	1.624	1.624	1.620
	(2)	1.629	1.622	1.626	1.625	1.624	1.625	1.622	1.621
T(2)-O(4)	obs	1.609	1.604(4)	1.594(6)	1.594(3)	1.586(2)	1.578(5)	1.572(7)	1.587(3)
	(1)	1.594	1.594	1.598	1.594	1.590	1.593	1.593	1.590
	(2)	1.599	1.592	1.596	1.595	1.594	1.594	1.591	1.591
T(2)-O(5)	obs	1.639	1.611(5)	1.637(7)	1.634(3)	1.653(2)	1.658(7)	1.660(8)	1.648(4)
	(1)	1.624	1.624	1.643	1.624	1.651	1.662	1.662	1.651
	(2)	1.629	1.622	1.641	1.625	1.655	1.663	1.660	1.652
T(2)-O(6)	obs	1.643	1.638(5)	1.654(7)	1.655(4)	1.672(2)	1.681(6)	1.674(7)	1.659(3)
	(1)	1.654	1.654	1.643	1.654	1.651	1.662	1.662	1.651
	(2)	1.659	1.652	1.641	1.655	1.655	1.663	1.660	1.652
<T(2)-O>	obs	1.629	1.622	1.626	1.625	1.632	1.636	1.633	1.629
	(1)	1.624	1.624	1.628	1.624	1.628	1.635	1.635	1.628

*method (1) is where <Si-O> is estimated from the equation of Brown & Gibbs (1969); method (2) uses the observed <Si-O> distance.

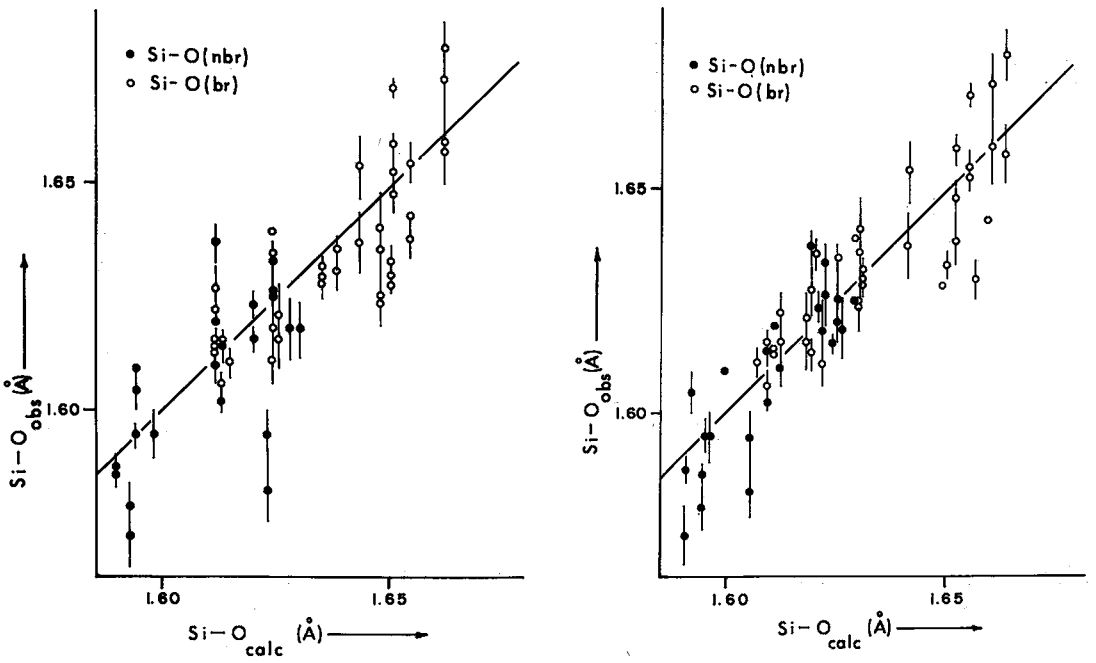

FIG. 36. Comparison of observed Si–O bond-lengths in $C2/m$ amphiboles (with little or no ^{IV}Al) with values calculated according to the methods of Baur (1970, 1971). The left-hand graph shows values calculated using predicted <Si–O> distances and the right-hand graph shows values calculated using observed <Si–O> distances.

TABLE 19. EMPIRICAL BOND-VALENCE (V.U.) TABLES FOR SELECTED NON-ALUMINOUS *C2/m* AMPHIBOLES

	M(1)	M(2)	M(3)	M(4)	A	T(1)	T(2)	Σ	Σ^p
Cummingtonite (21): r.m.s. deviations are 3.2% and 9.6% respectively									
O(1)	0.375	0.312	0.346$\downarrow^{X2}$			1.008		2.041	2.000
O(2)	0.325	0.347		0.333			0.992	1.997	2.000
O(3)	0.353$\downarrow^{X2}$		0.367					1.073	1.000
O(4)		0.386		0.480			1.035	1.901	1.667
O(5)				(0.045)		1.021	0.956	1.977	2.000
O(6)				0.107		0.984	0.946	2.037	2.333
O(7)						1.024$\downarrow^{X2}$		2.048	2.000
Σ	2.106	2.090	2.160	1.840		4.037	3.929		
Glaucophane (26): r.m.s.deviations are 4.2% and 9.2% respectively									
O(1)	0.355	0.384	0.343$\downarrow^{X2}$			1.011		2.093	2.167
O(2)	0.352	0.474		0.185			1.011	2.022	1.958
O(3)	0.338$\downarrow^{X2}$		0.364					1.040	1.000
O(4)		0.591		0.212			1.078	1.881	1.625
O(5)				0.097		1.016	0.961	2.074	2.125
O(6)				0.173		1.003	0.920	2.096	2.125
O(7)						1.030$\downarrow^{X2}$		2.060	2.000
Σ	2.090	2.898	2.100	1.334		4.060	3.970		
Tremolite (30): r.m.s. deviations are 4.4% and 11.3% respectively									
O(1)	0.356	0.309	0.351$\downarrow^{X2}$			1.055		2.071	2.000
O(2)	0.345	0.342		0.287			1.016	1.990	1.917
O(3)	0.342$\downarrow^{X2}$		0.361					1.064	1.000
O(4)		0.395		0.341			1.101	1.837	1.583
O(5)				0.133		0.974	0.922	2.029	2.250
O(6)				0.211		0.982	0.878	2.071	2.250
O(7)						1.016$\downarrow^{X2}$		2.032	2.000
Σ	2.086	2.092	2.146	1.944		4.027	3.917		
Fluor-tremolite (36): r.m.s. deviations are 6.8% and 11.3% respectively									
O(1)	0.359	0.301	0.362$\downarrow^{X2}$			1.021		2.043	2.000
O(2)	0.363	0.346		0.291			0.997	1.997	1.917
O(3)	0.282$\downarrow^{X2}$		0.311					0.818	1.000
O(4)		0.387		0.359			1.098	1.844	1.583
O(5)				0.138		0.984	0.934	2.056	2.250
O(6)				0.226		0.979	0.908	2.113	2.250
O(7)						1.043$\downarrow^{X2}$		2.086	2.000
Σ	1.980	2.068	2.012	2.028		4.027	3.937		

	M(1)	M(2)	M(3)	M(4)	A	T(1)	T(2)	Σ	Σ^p
Grunerite (22): r.m.s. deviations are 1.6% and 9.6 respectively									
O(1)	0.393	0.319	0.361$\downarrow^{X2}$			0.961		2.034	2.000
O(2)	0.322	0.346		0.350			0.971	1.989	2.000
O(3)	0.334$\downarrow^{X2}$		0.353					1.021	1.000
O(4)		0.395		0.516			1.049	1.960	1.667
O(5)				(0.033)		0.987	1.030	2.017	2.000
O(6)				0.086		0.979	0.959	2.024	2.333
O(7)						1.024$\downarrow^{X2}$		2.048	2.000
Σ	2.098	2.120	2.150	1.904		3.951	4.009		
Tirodite (28): r.m.s. deviations are 3.4% and 9.6% respectively									
O(1)	0.371	0.308	0.347$\downarrow^{X2}$			1.032		2.058	2.000
O(2)	0.330	0.346		0.327			1.011	2.014	2.000
O(3)	0.354$\downarrow^{X2}$		0.367					1.075	1.000
O(4)		0.402		0.419			1.078	1.899	1.667
O(5)				(0.050)		1.000	0.969	1.969	2.000
O(6)				0.134		0.971	0.917	2.022	2.333
O(7)						0.016$\downarrow^{X2}$		2.032	2.000
Σ	2.110	2.112	2.122	1.760		4.019	3.975		
Fluor-richterite (34): r.m.s. deviations are 6.8% and 12.9% respectively									
O(1)	0.359	0.278	0.351$\downarrow^{X2}$			1.113		2.101	2.000
O(2)	0.381	0.359		0.236			0.992	1.968	1.854
O(3)	0.276$\downarrow^{X2}$		0.300					0.852	1.000
O(4)		0.398		0.273			1.125	1.796	1.521
O(5)				0.103	0.087$\downarrow^{X2}$	0.992	0.910	2.092	2.271
O(6)				0.166	0.061$\downarrow^{X2}$	0.951	0.858	2.036	2.271
O(7)					0.182	0.964$\downarrow^{X2}$		2.110	2.200
Σ	2.032	2.070	2.004	1.556	0.956	4.020	3.885		
Ferro-glaucophane (69): r.m.s. deviations are 4.1% and 9.2% respectively									
O(1)	0.367	0.396	0.339$\downarrow^{X2}$			0.992		2.094	2.167
O(2)	0.361	0.476		0.193			0.977	1.947	1.958
O(3)	0.341$\downarrow^{X2}$		0.382					1.064	1.000
O(4)		0.605		0.220			1.072	1.897	1.625
O(5)				0.094		1.019	0.927	2.040	2.125
O(6)				0.175		0.997	0.917	2.089	2.125
O(7)						1.013$\downarrow^{X2}$		2.026	2.000
Σ	2.138	2.954	2.120	1.364		4.021	3.893		

valence rule (Baur 1970) quite well, and the predictive nature of this scheme promises to be useful in structure modeling by D.L.S. (distance least-squares: Meier & Villiger 1969) methods. Table 19 shows the results of a complete bond-valence analysis on eight clinoamphiboles containing little ^{IV}Al (<0.1 apfu), where the results are compared with the bond-strength sums calculated from the formal Pauling scheme. It is apparent that the bond-length variations

observed in the refined structures tend to minimize the deviations from ideality in the bond-valence sums around the anions. This is of particular significance with respect to cations co-ordinating the O(4) anion, all of which show extremely short bonds to O(4). Thus in the clinoamphiboles, T(2)–O(4) generally is shorter or equal to 1.60 Å, no matter what other variations in chemistry or structure (or both) occur. In order to maintain a mean bond-length in accord with the size of its constituent cation (Si), there is a concomitant lengthening of the other bonds. As a result of this, T(2) is generally the more distorted of the two tetrahedra.

Shannon (1975, 1976), Brown & Shannon (1973) and Brown (1978) have shown that variation in mean bond-length for a specific cation–anion pair can be significantly correlated with polyhedron distortion Δ, and that this can be interpreted in terms of the shape of bond-length *vs.* bond-valence curves. In the non-^{iv}Al amphiboles, <T(2)–O> varies between 1.622 and 1.636 Å, and Hawthorne (1976) showed that this variation correlates with Δ. Figure 37 shows the relation between mean bond-length and Δ for *C*2/*m* amphibole tetrahedra containing little or no Al. Although the correlation is well developed, its significance is not clear as the factors affecting mean bond-lengths in tetrahedral oxyanions are not well understood. Calculation of the ideal relationship from the Si–O bond-valence curve of Brown & Shannon (1973) suggests that distortion variations should not contribute significantly to variations in <T–O> in amphiboles. Baur (1974) has shown that ^{iv}<P–O> is significantly correlated with tetrahedral distortion. Conversely, Baur (1978) showed that <Si–O> in a large number (314) of silicate tetrahedra was not significantly correlated with tetrahedral distortion but was a linear function of the number of O(br) anions per tetrahedron and the mean co-ordination number of all O atoms within the tetrahedron. This would suggest that the correlation of Figure 37 is spurious, whereas the phosphate study (Baur 1974) could be taken as supporting this correlation. As indicated earlier, an argument based on the covalent model for the Si–O bond has been put forward (Mitchell *et al.* 1971) to rationalize the same trend. However, this figure has considerable implication concerning the derivation of Al/Si site-occupancies (Hawthorne 1976) and is perhaps best considered as an empirical correlation at present.

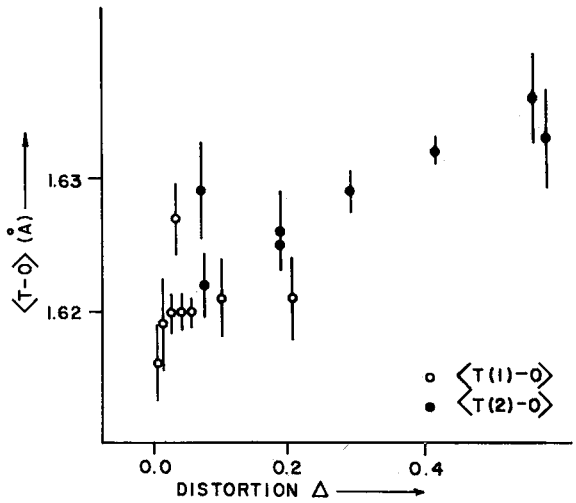

FIG. 37. Variation in mean bond-length as a function of polyhedral distortion parameter Δ for *C*2/*m* amphiboles with ^{iv}Al less than 0.10 a.p.f.u.

The P2₁/m amphiboles

There are four unique cation-sites with pseudotetrahedral co-ordination in this structure, the T(1A), T(2A), T(1B) and T(2B) sites. Figure 12 shows details of their co-ordination. The T(1A) tetrahedron shares one corner with an adjacent T(1A) tetrahedron, one corner with an adjacent T(2A) tetrahedron, one corner with the other adjacent T(2A) tetrahedron and with a [6]-co-ordinate M(4) polyhedron, and the fourth corner with the M(1), M(2) and M(3) octahedra; furthermore, it shares one edge with an [8]-co-ordinate M(4) polyhedron. The T(2A) tetrahedron shares one corner with an adjacent T(1A) tetrahedron, one corner with the other adjacent T(1A) tetrahedron and with an [8]-co-ordinate M(4) polyhedron, one corner with the M(2) octahedron and a fourth corner with the M(1), M(2) and M(4) polyhedra; in addition, it shares one edge with the M(4) polyhedron. The environments of the B tetrahedra are topologically similar to the corresponding A tetrahedra described above.

Papike *et al.* (1969) have shown that the "average structure" of this amphibole is very similar to tirodite(28), and hence this amphibole will behave as tirodite in all correlations involving average parameters (see previous section on *C*2/*m* amphiboles). With regard to individual bond-lengths, T–O(br) tends to be longer than T–O(nbr), although there is some overlap of the values. Similarly, there is a *tendency* for the bond angles to order themselves in the sequence O(nbr)–T–O(nbr)>O(br)–T–O(nbr)>O(br)–T–O(br), thus showing a qualitative agreement with the predictions of

TABLE 20. BOND-VALENCE TABLE FOR CUMMINGTONITE $P2_1/m$(27)

	M(1)	M(2)	M(3)	M(4)	T(1A)	T(2A)	T(1B)	T(2B)		
O(1A)	0.352	0.308	0.337 ↓x2		1.089				2.086	
O(2A)	0.315	0.362		0.337		0.995			2.009	
O(3A)	0.346 ↕x2		0.372						1.064	
O(4A)		0.395		0.386		1.134			1.915	
O(5A)				(0.048)	1.041	0.961			2.002	(2.050)
O(6A)				0.168	1.016	0.869			2.053	
O(7A)					0.984 ↕x2				1.968	
O(1B)	0.368	0.303	0.351 ↕x2				1.003		2.025	
O(2B)	0.335	0.326		0.327				1.035	2.023	
O(3B)	0.348 ↕x2		0.347						1.043	
O(4B)		0.396		0.454				1.032	1.882	
O(5B)				(0.075)			0.969	0.966	1.935	(2.010)
O(6B)				0.127			0.964	0.966	2.057	
O(7B)							1.052 ↕x2		2.104	
Σ	2.064	2.090	2.095	1.799 VI, 1.874 VII, 1.922 VIII	4.130	3.959	3.988	3.999		
Ideal charge	2.00	2.00	2.00	2.00	4.00	4.00	4.00	4.00		

molecular orbital theory. Examination of the bond-valence distributions in the tetrahedral part of the structure (Table 20) shows that the tetrahedral bond-length variations may be adequately rationalized using a bond-valence model. As with other amphibole types, the O(4A) and O(4B) anions play a major role in controlling bond-length variations. In the A chain, T(2A)–O(4A) is very short and the T(2A)–O(br) bonds are long in order to compensate for this. This effect is less important in the B chain, where the M(4) cation(s) contribute a much greater bond-valence than in the A chain; accordingly, T(2B)–O(4B)>T(2A)–O(4A) and hence, the T(2B) tetrahedron, are far less distorted than the T(2A) tetrahedron. It is of interest to note that the distribution of bond valences in the tetrahedral double-chains is compatible with the changes in M(4) environment that are thought to reflect the entry of considerable amounts of Mg into M(4) and cause the $P2_1/m$ structure to occur.

The P2/a amphiboles

There are four unique cation-sites with pseudotetrahedral co-ordination, the T(1)A, T(2)A, T(1)B and T(2)B sites. Figure 13 shows details of their co-ordination. The T(1)A tetrahedron shares one corner with an adjacent T(1)B tetrahedron, two corners with adjacent T(2)A tetrahedra, one corner with the M(1)A, M(2)A and M(3) octahedra and one edge with the M(4)A polyhedron. The T(2)A tetrahedron shares two corners with adjacent T(1)A tetrahedra, one corner with the M(1)A, M(2)A and M(4)A polyhedra and one edge with the M(4)A polyhedron. The environments of the B tetrahedra are similar, with the additional feature that all bridging anions are also bonded to the A(2) cation.

The joesmithite structure shows reasonable correspondence with the predictions of a molecular orbital model; generally, one finds T–O(br) > T–O(nbr) and O(nbr)–T–O(nbr) > O(br)–T–O(nrb)>O(br)–T–O(br), although some discrepancies do occur. A bond-valence table is shown in Table 21; the much weaker Be bonds are compensated by the strong bonds of the divalent A(2) cation to the bridging oxygens together with the strong M(4)B–O(5)B bond (0.226 as compared with 0.133 v.u. in tremolite). The bond-valence requirements of the O(4)A and O(4)B anions are also a major factor in tetrahedral bond-length variations, but do not play quite as dominant a role as normal because of the unusual chemistry.

The Pnma amphiboles

There are four unique cations-sites with pseudotetrahedral co-ordination in this structure-type, the T1A, T2A, T1B and T2B sites; Figure 14 shows details of their co-ordination. The T1A tetrahedron shares one corner with an adjacent T1A tetrahedron, one corner with an adjacent T2A tetrahedron and with a [6]-co-ordinate M4 polyhedron, one corner with the

TABLE 21. EMPIRICAL BOND-VALENCE TABLE FOR JOESMITHITE(25)

	M(1)A	M(2)A	M(1)B	M(2)B	M(3)	M(4)A	M(4)B	A(2)	T(1)A	T(2)A	T(1)B	T(2)B	Σ
O(1)A	0.368	0.348			0.315				1.107				2.138
O(2)A	0.362	0.367				0.277				1.016			2.022
O(1)B			0.471	0.484	0.392						0.500		1.847
O(2)B			0.385	0.461			0.219					0.956	2.021
O(3)	0.352		0.393		0.386								1.131
O(4)A		0.399				0.351				1.075			1.825
O(5)A						0.166			0.977	0.896			2.039
O(6)A						0.184			0.977	0.922			2.083
O(4)B				0.551			0.328					1.128	2.007
O(5)B							0.226	$0.242^{\times 2}_{\downarrow}$			0.458	0.924	1.850
O(6)B							0.214	$0.220^{\times 2}_{\downarrow}$			0.453	0.944	1.831
O(7)								$0.235^{\times 2}_{\downarrow}$	1.113		0.604		1.952
Σ*	2.164	2.228	2.498	2.992	2.186	1.956	1.974	$(1.394)^{VI}$	4.174	3.909	2.015	3.592	
Ideal charge	2.15	2.26	2.68	3.00	2.00	2.00	2.00	2.00	4.00	4.00	2.00	4.00	

*all M-site bond-valences (v.u.) have a multiplicity of 2 in the cation sum.

other adjacent T2A tetrahedron and with the A-site octahedron, and the fourth corner with the M1, M2 and M3 octahedra. The T2A tetrahedron shares one corner with an adjacent T1A tetrahedron and with the A-site octahedron, one corner with the other adjacent T1A tetrahedron and with a [6]-co-ordinate M4 polyhedron, one corner with the M2 and M4 polyhedra, and the fourth corner with the M1, M2 and M4 polyhedra. The environments of the B tetrahedra are topologically identical with the corresponding A tetrahedra.

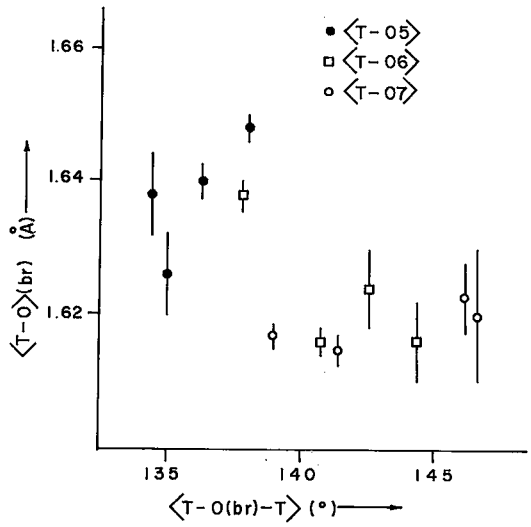

FIG. 38. Variation in individual <T–O(br)> as a function of individual <T–O(br)–T> for the *Pnma* amphiboles with little or no tetrahedrally co-ordinated Al.

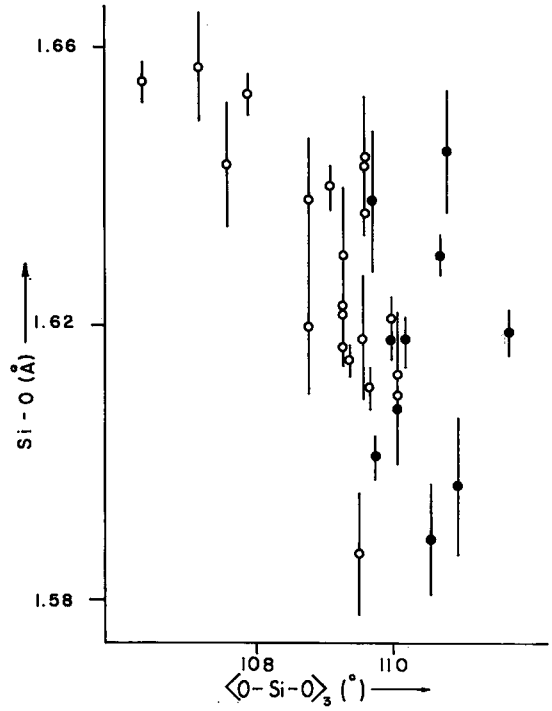

FIG. 39. Variation in individual Si–O bond-lengths as a function of the mean value of the three O–Si–O angles involved in that bond for the *Pnma* amphiboles with little or no tetrahedrally co-ordinated Al.

There is some tendency for shorter T–O(br) bonds to be associated with wider T–O(br)–T angles (Fig. 38), but as with the *C*2/*m* amphiboles, the correlation is not well developed. The

TABLE 22. EMPIRICAL BOND-VALENCE (V.U.) TABLE FOR SELECTED *Pnma* AMPHIBOLES

	M1	M2	M3	M4	T1A	T1B	T2A	T2B	Σ	Σ^p
Anthophyllite 23 : r.m.s. deviations are 4.4% and 8.0% respectively										
01A	0.365	0.304	0.354 ↓×2		1.011				2.034	1.995
01B	0.373	0.317	0.350 ↓×2			1.011			2.051	2.000
02A	0.324	0.360		0.318			1.008		2.010	2.061
02B	0.308	0.348		0.341				0.979	1.976	2.066
03A	0.348 ↓×2		0.371						1.067	1.000
03B	0.365 ↓×2		0.368						1.098	1.000
04A		0.415		0.422			1.057		1.894	1.728
04B		0.388		0.479				1.038	1.905	1.733
05A				0.185	0.954		0.917		2.056	2.390
05B				(0.070)		0.964		0.946	1.910	2.000
06A				(0.025)	1.030		1.003		2.033	1.990
06B				(0.070)		1.000		0.922	1.922	2.000
07A					1.019 ↓×2				2.038	1.990
07B						1.013 ↓×2			2.206	2.000
Σ	2.083	2.132	2.147	1.745	4.014	3.988	3.985	3.885		

	M1	M2	M3	M4	A	T1A	T1B	T2A	T2B	Σ	Σ^p
Gedrite 32 : r.m.s. deviations are 4.4% and 7.5% respectively											
01A	0.361	0.387	0.369 ↓×2			0.927				2.044	2.041
01B	0.372	0.407	0.338 ↓×2				0.893			2.010	2.034
02A	0.316	0.425		0.275				0.966		1.982	2.105
02B	0.298	0.393		0.356					0.934	1.981	2.073
03A	0.353 ↓×2		0.401							1.107	1.000
03B	0.366 ↓×2		0.396							1.128	1.000
04A		0.487		0.339				1.122		1.948	1.772
04B		0.458		0.438					0.979	1.875	1.740
05A				0.272				0.959		2.107	2.267
05B				0.181			0.910		0.882	2.015	2.228
06A				(0.020)	0.041 ↓×2	0.966		1.041		2.048	1.992
06B				(0.073)	0.041 ↓×2		0.920		0.951	1.912	1.953
07A					0.062	0.954 ↓×2				1.970	1.927
07B					0.076		0.946 ↓×2			1.968	1.913
Σ	2.066	2.557	2.211	1.861	0.304	3.723	3.669	4.088	3.746		

	M1	M2	M3	M4	T1A	T1B	T2A	T2B	Σ	Σ^p
Holmquistite 31 : r.m.s. deviations are 4.3% and 5.0% respectively										
01A	0.363	0.403	0.357 ↓×2		0.959				2.082	2.155
01B	0.369	0.389	0.352 ↓×2			0.979			2.089	2.166
02A	0.333	0.473		0.180			0.979		1.965	2.037
02B	0.333	0.476		0.193				0.941	1.943	2.037
03A	0.356 ↓×2		0.380						1.092	1.000
03B	0.356 ↓×2		0.387						1.099	1.000
04A		0.617		0.170			1.092		1.879	1.704
04B		0.598		0.211				1.069	1.878	1.704
05A				0.127	1.011		0.912		2.050	2.193
05B				(0.052)		1.024		0.959	1.983	2.000
06A				(0.024)	1.098		0.944		2.042	1.989
06B				(0.065		1.032		0.946	1.978	2.000
07A					0.997 ↓×2				1.994	1.978
07B						1.005 ↓×2			2.010	2.000
Σ	2.110	2.956	2.185	0.881	4.065	4.040	3.927	3.915		

	M1	M2	M3	M4	A	T1A	T1B	T2A	T2B	Σ	Σ^p
Gedrite 33 : r.m.s. deviations are 4.5% and 7.6% respectively											
01A	0.382	0.401	0.345 ↓×2			0.922				2.050	2.061
01B	0.384	0.413	0.336 ↓×2				0.862			1.995	2.018
02A	0.301	0.423		0.257				1.024		2.005	2.122
02B	0.307	0.423		0.352					0.854	1.936	2.055
03A	0.347 ↓×2		0.378							1.072	1.000
03B	0.374 ↓×2		0.384							1.132	1.000
04A		0.500		0.345				1.046		1.891	1.789
04B		0.470		0.453					0.954	1.877	1.722
05A				0.262		0.905		0.915		2.082	2.260
05B				0.190			0.867		0.862	1.919	2.150
06A				(0.016)	0.064 ↓×2	0.951		0.977		1.992	1.937
06B				(0.066)	0.064 ↓×2		0.887		0.905	1.856	1.827
07A					0.097	0.932 ↓×2				1.961	1.875
07B					0.106		0.892 ↓×2			1.890	1.789
Σ	2.095	2.630	2.124	1.859	0.459	3.710	3.508	3.962	3.575		

O–T–O angles do tend to decrease in the forecast order, but again there is considerable overlap among the different populations. Figure 39 shows the variation in T–O with $<O–T–O>_3$ for the non-^{iv}Al orthoamphiboles. As with the *C2/m* clinoamphiboles, the correlation is significant, indicating that at least part of the variation in Si–O distances can be rationalized in terms of a covalent bonding model.

An examination of tetrahedral bond-length variations in terms of bond valence is shown in Table 22. The results are very similar to those for the other amphibole types, confirming the importance of anion bond-strength requirements in controlling bond lengths and emphasizing the role of the O4A and O4B anions in constraining possible variations.

TABLE 23. EMPIRICAL BOND-VALENCE TABLE FOR PROTOAMPHIBOLE[20]

	M1	M2	M3	M4	A	T1	T2	Σ
O1	0.350	0.282	0.357 ↓x2			1.083		2.072
O2	0.334	0.341		0.289			1.046	2.010
O3	0.291 ↓x2		0.305					0.887
O4		0.417		0.339			1.083	1.839
O5					-	1.016	0.989	2.005
O6				0.151	-	0.997	0.917	2.065
O7					-	0.995 ↓x2		1.990
Σ	1.950	2.080	2.038	1.558[1]	-	4.091	4.035	

[1] ideal sum is 1.75 v.u. All M-site bond-valences (v.u.) have a multiplicity of 2 in the cation sum.

The Pnmn amphiboles

There are two unique cation-sites with pseudotetrahedral co-ordination in this structure-type, the T1 and T2 sites. Figure 15 shows details of their co-ordination. Both sites have point-symmetry 1 and are surrounded by four oxygen anions. The T1 tetrahedron shares one corner with an adjacent T1 tetrahedron, one corner with an adjacent T2 tetrahedron, one corner with the other adjacent T2 tetrahedron and with the [6]-co-ordinate M4 polyhedron, a fourth corner with the M1, M2 and M3 octahedra. The T2 tetrahedron shares two corners with adjacent T1 tetrahedra, one corner with the M2 octahedron, the fourth corner with the M1, M2 and M4 polyhedra and one edge with the [6]-co-ordinate M4 polyhedron.

In protoamphibole, T–O(br) is greater than T–O(nbr), and the angles of the T1 tetrahedron decrease in the predicted sequence O(nbr)–T–O(nbr) > O(br)–T–O(nbr) > O(br)–T–O(br). The angles of the T2 tetrahedron deviate somewhat from this sequence owing to perturbing electrostatic and geometrical factors. Possibly as a result of this, the T–O bond-lengths do not show good correlation with the $<O–T–O>_3$ angles (Gibbs 1969). The T2 tetrahedron shows a far greater range of O–T–O angles than the T1 tetrahedron, presumably the result of relaxation due to cation–cation repulsion across the shared edge between the T2 and M4 polyhedra.

A bond-valence analysis of protoamphibole [20] is shown in Table 23; as with the other structure types, anion bond-valence requirements are an important control on bond-length variations. All cations show extremely short bonds to O4. Thus the other bonds involving these cations have to lengthen in order to maintain ideal bond-valence sums at the cations. M2–O1 lengthens and T1–O1 accordingly shortens to maintain the required bond-valence sum around O1. Similarly, M4–O6 lengthens and the T–O6 bond-lengths presumably compensate for this. It is interesting to note that the expected decrease in T1–O6 bond-valence because of the presence of the M4–O6 bond occurs entirely in the T2–O6 bond, where it compensates for the increase in the bond valence of T2–O4.

The Tetrahedral Double-Chain in ^{iv}Al Amphiboles

The substitution of Al for Si in the tetrahedral double-chain of the amphiboles is a major factor in amphibole chemistry. Such chemical variations seem to be a function of both bulk-rock composition and intensive parameters at the time of equilibration. The Al content of the tetrahedral sites in the amphiboles varies between 0.0 and ~3.0 atoms p.f.u., although it should be noted that amphiboles in which tetrahedral Al exceeds ~2.0 atoms p.f.u. are rather uncommon (Appleyard 1975, Bunch & Okrusch 1973) and occur in silica-deficient environments.

Ordering of tetrahedrally co-ordinated Al

Aluminum is distributed over the crystallographically distinct tetrahedrally co-ordinated sites in the amphibole structures. Because the X-ray scattering factors of Al and Si are very similar, direct determination of site populations by least-squares refinement of single-crystal X-ray data is accompanied by high variable correlations and large standard deviations; in addition, the solution obtained is extremely sensitive to any systematic error present in the data. In principle, this problem may be alle-

viated somewhat by the use of high-angle X-ray data (Kosoi *et al.* 1974) or neutron data, but these methods have not yet been used in the refinement of ^{iv}Al-rich amphiboles. As the tetrahedral Al site-populations are of considerable interest, both with respect to the possible methods of local charge-balance and to their effect on the geometry of the tetrahedral double-chain, it would be of interest to confirm refined Al site-populations and to assign site populations for those structures where this was not done in the refinement procedure.

This problem was first examined by Papike & Clark (1967) and Papike *et al.* (1969). They described three methods by which tetrahedral Al site-populations could be obtained for clinoamphiboles: (i) <T–O> distances from a number of amphibole structures were used to set up a Smith–Bailey plot, resulting in the equation $0.128\ Al_T = <T\text{–}O>_T - 1.623$; (ii) the amount of Al determined by chemical analysis is assigned to each site by comparison of the <T–O> distances with those of tremolite (Papike *et al.* 1969), and (iii) <T–O(nbr)> distances are used as in method (ii).

They concluded that method (ii) gave the most consistent results, and this was supported by Robinson *et al.* (1973) and Hawthorne & Grundy (1973a, b). Robinson (1971) and Robinson *et al.* (1973) developed separate equations for predicting Al occupancy of T(1) and T(2) in C-centred clinoamphiboles by plotting the <T(1)–O> and <T(2)–O> distances against the refined Al site-occupancies, using data from five clinoamphiboles and a series of clinopyroxenes:

$$Al_{T(1)} = 760(77)\ <T(1)\text{–}O> - 1230(4) \qquad R = 0.98$$
$$Al_{T(2)} = 766(54)\ <T(2)\text{–}O> - 1248(2) \qquad R = 0.98.$$

Bocchio *et al.* (1978) proposed the following equation relating total ^{iv}Al per formula unit to the <T(1)–O> distance:

$$^{iv}Al\ (p.f.u.) = (<T(1)\text{–}O> - 1.620) \times 37.7$$

Here, it is assumed that there is no ^{iv}Al at the T(2) site [except in obvious examples such as subsilicic titanian magnesian hastingsite(58)]. Hawthorne & Grundy (1977a) showed that the grand <T–O> distance in a series of ten clinoamphiboles was linearly related to the tetrahedral Al per T(1) + T(2) site (^{iv}Al p.f.u./4.0) by the equation

$$Al_{TET} = 16.252<T\text{–}O> - 26.434 \qquad R = 0.997.$$

With the assumption that the slopes of the individual relationships for the T(1) and T(2) tetrahedra are the same, the following two equations relating <T(1)–O> and <T(2)–O> to the Al occupancies were derived:

$$Al_{T(1)} = 8.126<T(1)\text{–}O> - 13.170$$
$$Al_{T(2)} = 8.126<T(2)\text{–}O> - 13.262.$$

Hawthorne (1976) and Ungaretti (1980) suggested that variations in both individual and mean tetrahedral bond-lengths occur as a result of *other* cation substitutions in the structure; certainly in the non-^{iv}Al amphiboles, variations in individual <T–O> distances correlate with bond-length distortion Δ (Fig. 37) that changes as a result of nontetrahedral cation variation in the structure. Ungaretti (1980) suggested that much of the variation in <T(2)–O> in aluminous amphiboles is due to these other factors rather than to substitution of ^{iv}Al. This may well be the case; the T(2) equation may not be very reliable at small ^{iv}Al occupancies, but it should indicate where significant ^{iv}Al occupancy of T(2) does occur, as is the case for subsilicic titanian magnesian hastingsite(58). Figure 40 shows a comparison between the total Al p.f.u. and some of the equations given above. No matter which curve is considered, some scatter is encountered. Careful analysis of the data (Appendix B3) suggests that much of this scatter is due to poor or unrepresentative chemical data, although the perturbing effect of nontetrahedrally coordinated cations may be a contributing factor.

The primitive clinoamphiboles and the *Pnmn* orthoamphiboles contain little or no tetrahedral Al, and thus the question of tetrahedral Al ordering does not arise. The natural orthorhombic (*Pnma*) amphiboles may contain up to ~2.25 tetrahedral Al p.f.u., and this is distributed over the four unique tetrahedral sites in the structure. Papike & Ross (1970) used "method 2" of Papike *et al.* (1969) for assigning tetrahedral Al in two specimens of gedrite, but there has been no systematic examination of tetrahedral Al in orthorhombic amphiboles. Table 24 summarizes the available data. Figure 40 shows the variation in grand <T–O> distance with the amount of tetrahedral Al per unique tetrahedral site in the structure; the trend is distinctly nonlinear. However, comparison with the analogous relationship for the monoclinic amphiboles (Hawthorne & Grundy 1977a) shows three of the four datapoints to be collinear, defining a trend parallel to that of the monoclinic amphiboles but displaced downward by ~0.004 Å (Fig. 40). The values for gedrite[32] deviate by ~0.007 Å

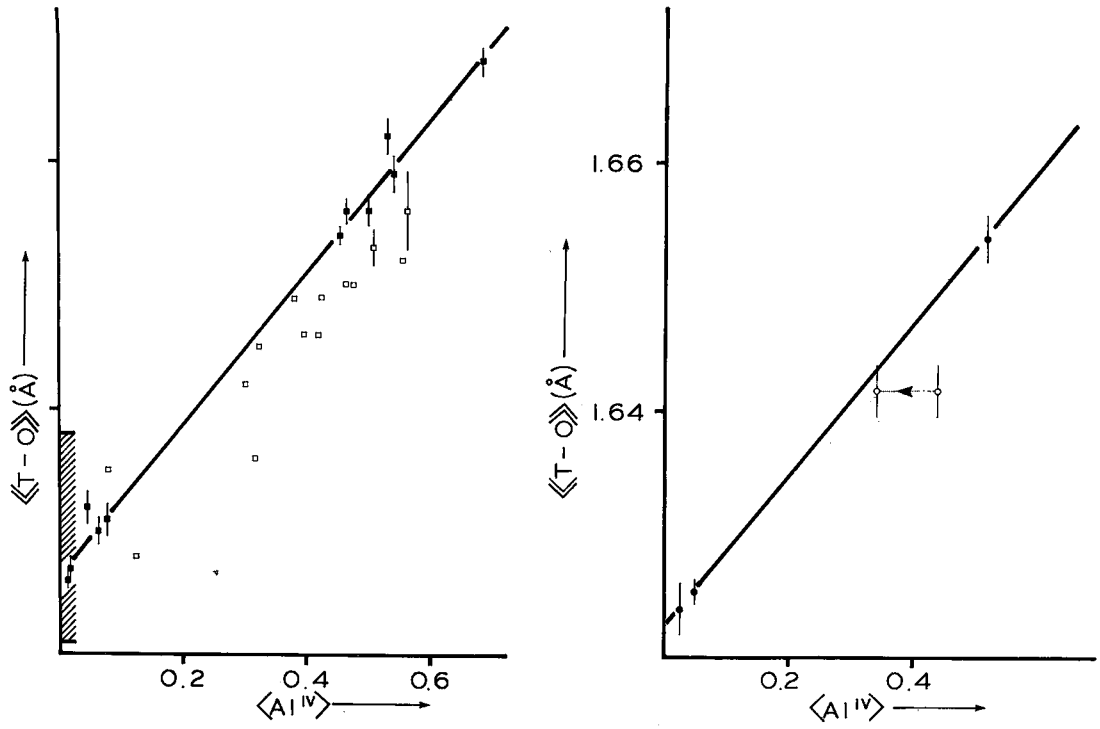

FIG. 40. Variation in grand <T–O> distance with total ^{IV}Al per T(1)+T(2) site in the *C*2/*m* amphiboles (left) and *Pnma* amphiboles (right). For the *C*2/*m* amphiboles, the hatched region shows the range of <T–O> values observed for amphiboles with ^{IV}Al ≃ 0 (see Fig. 37); the variation in this region correlates with polyhedron distortion. The solid line and solid squares are from Hawthorne & Grundy (1977a); the hollow squares represent additional data, many of which are of lower accuracy. For the *Pnma* amphiboles, the full line is drawn parallel to the trend for the *C*2/*m* amphiboles, through the three data-points shown; the point for gedrite [32] was modified as indicated in Appendix C.

TABLE 24. MEAN BOND-LENGTHS (Å) AND TETRAHEDRAL ALUMINUM IN *Pnma* AMPHIBOLES

	<T-O>	^{iv}Al	<T(1A)-O>	<T(1B)-O>	<T(2A)-O>	<T(2B)-O>
Anthophyllite[23]	1.625(1)	0.033	1.621(2)	1.623(2)	1.624(2)	1.634(2)
Holmquistite[31]	1.624(2)	0.023	1.617(4)	1.618(5)	1.630(4)	1.631(5)
Gedrite[32]	1.642(2)	0.438	1.650(4)	1.655(4)	1.615(4)	1.647(4)
Gedrite[33]	1.654(2)	0.512	1.651(4)	1.673(4)	1.626(4)	1.666(4)

^{iv}Al = ^{iv}Al p.f.u./4.0

or ~0.12Al from this relationship. Papike & Ross (1970) noted that the Na content of the A site in this gedrite (0.45 from the chemical analysis) led to an A-site temperature factor much larger than expected, and that refinement of the A-site occupancy produced a drop to 0.34 together with a reasonable isotropic temperature-factor: Papike & Ross (1970) preferred the values derived from the unconstrained structure-refinement to the results of the chemical analysis. This means that the remainder of the cell contents of this gedrite must be modified in order for electroneutrality to be maintained. Robinson *et al.* (1971) have suggested that the anthophyllite–gedrite series of amphiboles is a solid solution between two end-compositions $R^{2+}{}_2R^{2+}{}_5Si_8O_{22}(OH)_2$ and $Na_{0.5}R^{2+}{}_2R^{2+}{}_{3.5}R^{2+}{}_{1.5}Si_6Al_2O_{22}(OH)_2$. This being the case, an A-site occupancy of (0.34 Na + 0.66□) corresponds to a tetrahedral Al content of 1.36 atoms p.f.u. instead of the value 1.75 atoms p.f.u. indicated by the chemical analysis. As indicated in Figure

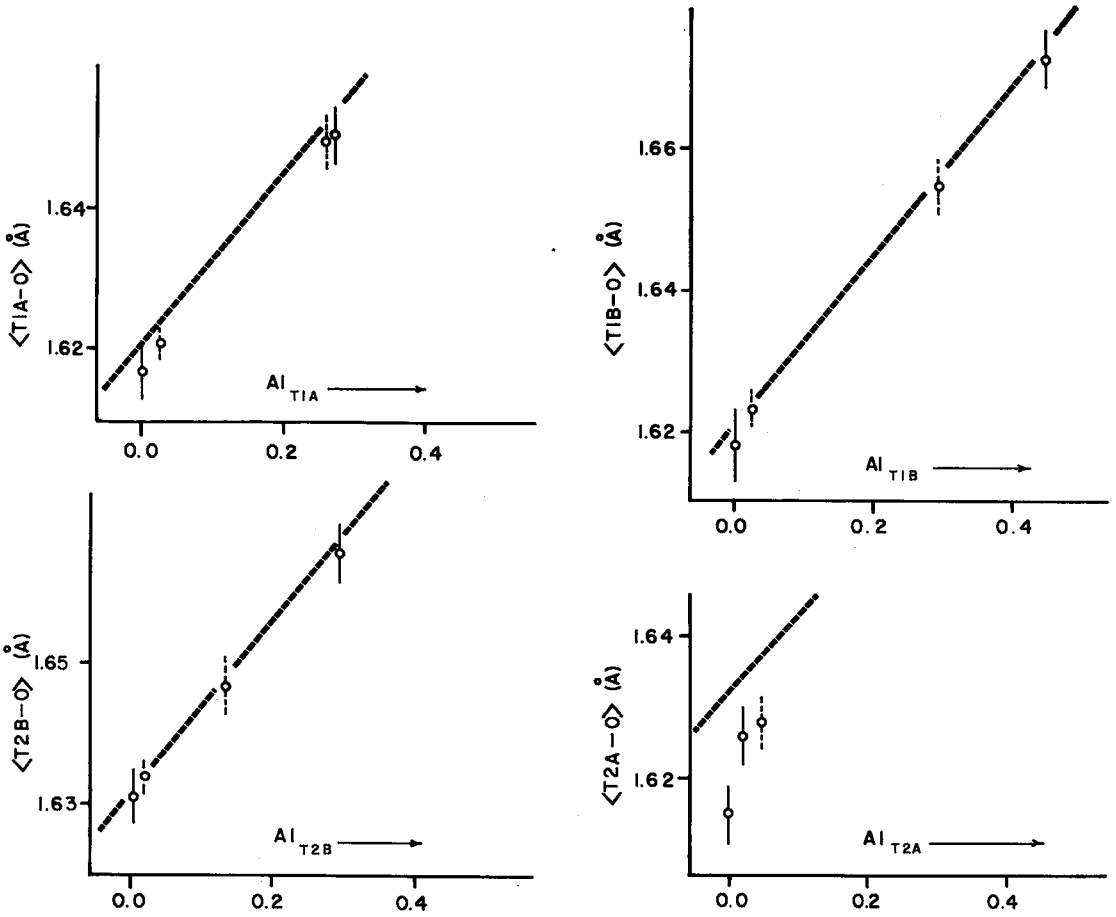

FIG. 41. Variation in individual <T–O> distances with constituent Al site-occupancies in the *Pnma* amphiboles; the broken lines are the individual relationships for the T(1) and T(2) sites in the *C*2/*m* amphiboles (Hawthorne & Grundy 1977a).

40, this value does not deviate significantly from the trend defined by the other three data-points. As the value for tetrahedral Al for gedrite[32] is not known very accurately and as there are only three other data-points, a linear regression analysis for Figure 40 was not performed. An interim working-curve may be derived by subtracting 0.004 Å from the curve for the monoclinic amphiboles, as shown by the unbroken curve in Figure 40.

The assignment of Al to the four unique tetrahedral sites was accomplished in the following manner. The behavior of the individual tetrahedra with regard to changing mean bond-length and Al/Si occupancy was assumed to be *similar* to that in the monoclinic amphiboles: thus, mean bond-length – Al content curves will be parallel but not necessarily coincident for both structure-types. This assumption is supported by the relationship exhibited in Figure 41. The values assigned for gedrite[33] (Papike & Ross 1970) agree closely with the curves for the monoclinic amphiboles. The most significant difference occurs for the T2A tetrahedron, where the mean bond-length is significantly less than that indicated by the curve for the T(2) tetrahedron in the monoclinic amphiboles. However, the latter statement applies to most of the orthorhombic amphiboles. For holmquistite[31], the mean tetrahedral bond-lengths are smaller than for all the other orthorhombic amphiboles except for the T2A tetrahedron; thus, all tetrahedral Al was assumed (tentatively) to be ordered in the T2A tetrahedron in holmquistite[31]. Tetrahedral site-populations for anthophyllite[23] and gedrite[32]

TABLE 25. PREDICTIVE EQUATIONS FOR ^{iv}Al IN THE *Pnma* AMPHIBOLES

$$Al^{TOT} = -26.368 + 16.252\langle\langle T\text{-}O\rangle\rangle$$

T1A	$Al = -13.146 + 8.126\langle T1A\text{-}O\rangle$	T2A	$Al = -13.175 + 8.126\langle T2A\text{-}O\rangle$
T1B	$Al = -13.157 + 8.126\langle T1B\text{-}O\rangle$	T2B	$Al = -13.257 + 8.126\langle T2B\text{-}O\rangle$

$Al = {}^{iv}Al$ p.f.u./4.0

were assigned by assuming linearity between holmquistite[31] and gedrite[33] in Figure 41, with the exception of T2A, for which gedrite[32] was assumed to have zero Al occupancy. The site occupancies assigned for anthophyllite[23] and gedrite[32] are supported by the fact that the total site-chemistry agrees with the corresponding values derived from the chemical analysis (anthophyllite[23]) and estimated from the refined value of the A-site Na (gedrite[32]). In view of the limited data-set, regression analyses were not performed; preliminary working-curves (Fig. 41) were derived by shifting the monoclinic amphibole curves down to correspond to the orthorhombic data to give the equations listed in Table 25.

All the methods outlined above have depended on ionic size as a criterion for the detection of Al/Si ordering. However, the bond-strength curves of Brown & Shannon (1973) may be used to assign site occupancies, and good agreement with the results of neutron diffraction experiments were obtained for sanidine (Brown & Shannon 1973, p. 277). As a part of this study, this approach was tried for the amphiboles of Appendices B and C, with the total amount of tetrahedral Al indicated by the chemical analysis as a check on the total tetrahedral Al indicated by the bond-valence calculations. Using the universal curves of Brown & Shannon (1973), the agreement was found to be poor; the tetrahedral Al was overestimated [*e.g.*, obs = 0.34, calc = 0.62 atoms p.f.u. for manganoan ferroactinolite(37); obs = 2.73, calc = 3.57 atoms p.f.u. for subsilicic titanian magnesian hastingsite(58)] and in synthetic nonaluminous amphiboles, up to 0.38 Al p.f.u. [fluor-richterite(34)] was calculated. Results were improved somewhat by the use of the "co-ordination corrected" curves of Brown & Shannon (1973). However, co-ordination numbers are sometimes difficult to decide convincingly, particularly when the next-nearest-neighbor cations are positionally disordered, the site is only partly occupied and the bonding contacts are at the margin of significance. In view of the reasonably satisfactory nature of the bond length *vs.* occupancy curves given above, this approach was not pursued further.

Stereochemistry of the double chain

As was shown in the previous section on model structures, increasing substitution of Al at the tetrahedral sites is accompanied by increased rotation of the tetrahedra of the double chain toward an O-rotated configuration in order to maintain linkage between the tetrahedral chain and octahedral strip parts of the structure. Substitution of Al at the tetrahedral sites is accompanied by balancing substitutions in other parts of the structure. The combination of these substitutions must be accompanied by stereochemical adjustments that allow the bond-valence requirements of the anions to be satisfied. The way in which this is done is apparent from the bond-valence tables for selected amphiboles shown in Table 26. The discussion on bond-length variations in non-^{iv}Al amphiboles emphasized the role of the O(4) anion; it is apparent from Table 26 that the same bond-valence constraints are operative in the ^{iv}Al amphiboles. Bond valences to the O(4) anion must be maintained at high values; thus ^{iv}Al will tend to avoid sites bonded to O(4) and order at sites not bonded to O(4). This is the case in the amphiboles of Table 26, where it can be seen that the bond valence of the T(2)–O(4) bond is the largest in the structure of each amphibole. The decrease in bond valence contributed to the anions co-ordinating the T(1) site is compensated for by the substitution of higher-valence cations at the other sites co-ordinated to these anions, and also by a strengthening of the M(4)–O(br) bonds that is promoted by the increased O-rotation of the double chain described above.

The Octahedral Strip

Sandwiched between opposing tetrahedral double-chains is the octahedral strip, an array of pseudo-octahedrally co-ordinated cation sites that are occupied by the C-type cations of the formula unit. This is the most compliant part of the amphibole structure, accepting cations that